

The Dynamic Nitric Oxide Pattern in Developing Cuttlefish *Sepia Officinalis*

Teresa Mattiello,¹ Maria Costantini,¹ Bruna Di Matteo,¹ Sonia Livigni,¹
Aude Andouche,² Laure Bonnaud,^{2,3} and Anna Palumbo^{1*}

Background: Nitric oxide (NO) is implied in many important biological processes in all metazoans from porifera to chordates. In the cuttlefish *Sepia officinalis* NO plays a key role in the defense system and neurotransmission. **Results:** Here, we detected for the first time NO, NO synthase (NOS) and transcript levels during the development of *S. officinalis*. The spatial pattern of NO and NOS is very dynamic, it begins during organogenesis in ganglia and epithelial tissues, as well as in sensory cells. At later stages, NO and NOS appear in organs and/or structures, including Hoyle organ, gills and suckers. Temporal expression of NOS, followed by real-time PCR, changes during development reaching the maximum level of expression at stage 26. **Conclusions:** Overall these data suggest the involvement of NO during cuttlefish development in different fundamental processes, such as differentiation of neural and nonneural structures, ciliary beating, sensory cell maintaining, and organ functioning. *Developmental Dynamics* 241:390–402, 2012. © 2012 Wiley Periodicals, Inc.

Key words: nitric oxide; nitric oxide synthase; *Sepia officinalis* development

Key findings:

- NO is endogenously synthesized in all developmental stages of the cuttlefish *Sepia officinalis*.
- The spatial pattern of NO and NOS is very dynamic and concerns both superficial and internal structures.
- NO could be involved in important functional processes providing new insights in this emerging model for developmental studies.

Accepted 30 November 2011

INTRODUCTION

Nitric oxide (NO) is an important physiological messenger produced by oxidation of L-arginine catalyzed by the enzyme NO synthase (NOS). NO and NOS are present in all metazoans from placozoans to vertebrates (Palumbo, 2005; Andreakis et al., 2011). Despite being a simple molecule, NO is a fundamental player in the fields of neuroscience, physiology and immunology. In nonvertebrates, NO

is suggested in many processes, including feeding, environmental stress, defense, blood sucking, bioluminescence, neural transmission, blood pressure regulation, immune response, swimming, regeneration processes (Palumbo, 2005; Palumbo and d'Ischia, 2007; Colasanti et al., 2010).

In the cuttlefish *Sepia officinalis*, NO plays a key role in the defense system, regulating the metabolism of

the ink gland and the activity of chromatophores (Palumbo et al., 2000; Fiore et al., 2004; Mattiello et al., 2010). Moreover, NO functions as neurotransmitter in the central and peripheral nervous system, regulates blood pressure acting as vasodilatory mediator, modulates the statocyst activity and participates in manipulative behavior (Schipp and Gebauer, 1999; Palumbo et al., 1999; Tu and Budelmann, 2000; Di Cosmo et al.,

¹Laboratory of Cellular and Developmental Biology, Stazione Zoologica Anton Dohrn, Naples, Italy

²Laboratory Biologie des Organismes Aquatiques et Ecosystèmes, UMR CNRS 7208, Museum National d'Histoire Naturelle, DMPA, Paris, France

³Univ Paris Diderot, Sorbonne Paris Cité Paris, France

Grant sponsor: ASSEMBLE Grant Agreement; Grant number: 227799.

*Correspondence to: Anna Palumbo, Laboratory of Cellular and Developmental Biology, Stazione Zoologica Anton Dohrn, Villa Comunale, 80121 Naples, Italy. E-mail: palumbo@szn.it

DOI 10.1002/dvdy.23722

Published online 3 January 2012 in Wiley Online Library (wileyonlinelibrary.com).

2000; Halm et al., 2003; Di Cristo et al., 2007).

Increasing evidence indicates that the role of NO is not only limited to adult metazoans. In vertebrates NO has been shown to affect a variety of processes, including neuron morphogenesis in zebrafish, cell proliferation and movements in *Xenopus*, preimplantation embryo development in mouse (Tranguch et al., 2003; Peunova et al., 2007; Bradley et al., 2010). Regarding lophotrochozoan mollusca scattered observation from the literature indicates the involvement of NO in developmental processes in gastropods. In particular, in the pond snail *Lymnaea stagnalis* NO regulates feeding activity, locomotion and heartbeat during embryonic development (Serfözö and Elekes, 2002). In *Helisoma trivolvis* NO stimulates in early embryonic development ciliary beating of embryos within the egg capsule (Cole et al., 2002). NO is also involved in neuronal development in some molluscs (Thavaradhara and Leise, 2001; Welshhans and Rehder, 2007) as well as in echinoderms (Bishop and Brandhorst, 2007). Moreover, NO is involved in different steps of the biological cycle, from fertilization to metamorphosis. In sea urchins, NO is produced in sea urchin eggs at fertilization, where it mobilizes intracellular calcium stores, regulates the duration of calcium transient and fertilization envelope hardening (Willmott et al., 1996; Leckie et al., 2003; Mohri et al., 2008). In the same time, NO regulates metamorphosis of sea urchins, ascidians and mollusc gastropods (Froggett and Leise, 1999; Bishop and Brandhorst, 2001, 2003; Bishop et al., 2001, 2008; Leise et al., 2004; Hens et al., 2006; Comes et al., 2007; Pechenik et al., 2007). In mollusc cephalopods, the development is direct, without any metamorphosis phase and up to now no information is available on the role of NO during development in such embryos that are protected by envelopes until hatching where they resemble an adult. The cuttlefish *Sepia officinalis* represents an emerging model for developmental studies for its biological features, wide natural distribution, commercial value and increasing availability of molecular biology tools. The direct development of *Sepia* offers the advantage to follow

the continuity of developmental processes; i.e., without changes of body plan as in most other mollusc species. In numerous gastropods, that have a trochophore larvae stage, deep modifications of systems (e.g., nervous and digestive) and molecular processes underlying them occur. Moreover, the originality and differences in gene/protein expression and in the molecular pathways have allowed to evidence specificities in the molecular networks implied in the development of this species. The studies on the expression patterns of *NK4*, *engrailed*, *Shh*, *Pax6* genes during *Sepia* development have provided some insights into nervous system differentiation, organization of the mantle, muscle formation and development (Baratte et al., 2007; Navet et al., 2008, 2009; Grimaldi et al., 2008). Recently, the expression of branchial acid-base transporters has been followed during development and in response to environmental hypercapnia (Hu et al., 2011). In *S. officinalis* characterized by several morphological peculiarities within mollusc and a direct development, we report the presence of NO in embryos by detecting NO and NOS enzyme and by monitoring *NOS* expression levels during the various developmental stages.

RESULTS

S. officinalis Development

S. officinalis develops directly without larval stage and metamorphosis. Development takes around 2 months at 20°C and 30 stages are characterized (Lemaire, 1970). Organogenesis proceeds during 2 to 3 weeks, from stage 14 to hatching at stage 30, giving rise to a juvenile identical to adult with a necto-benthic mode of life (Boletzky et al., 2006). From fertilization to stage 12, a discoidal cleavage at the animal pole of the egg leads to an embryo shaped as a disk lying on the yolk mass. At stage 14, the organogenesis begins: mantle with a central invagination initiating the shell sac responsible of the shell formation, optic vesicle, arm buds are delimited (Lemaire, 1970; Naef, 1928). At stage 17–18, the development of the visceral mass beneath the shell sac provokes the inflation of the mantle region. In the same time all the nerv-

ous ganglia differentiate in distinct area of the embryo (Fig. 1A). At stage 20, gills are covered by the mantle in the pallial cavity, the shell sac is closed. From stage 21, the cephalopodium inflates as most embryonic ganglia converge and become the prospective brain lobes (Fig. 1B). The adult shape is reached at around stage 22 (Fig. 1C). The future visceropallium (mantle, visceral mass, funnel, and mantle cavity) acquires a posterior position by sorting out of the embryo and the future cephalopodium (the prospective head and arms) congregates in an anterior position. The arms and tentacles grow and the suckers differentiate. The brain is constituted from differentiated lobes and located either in the supraesophageal part or in the subesophageal part; it is strikingly linked to the optic lobes (Fig. 1D).

Dynamic NO and NOS Detection Patterns in *S. officinalis* Embryos

The endogenous NO localization during development was evaluated using DAF-FM-DA, a sensitive cell-permeable and nonfluorescent reagent that combines with the NO oxidation product N_2O_3 to form a fluorescent benzotriazole. This probe is commonly used for imaging intracellular NO in biological systems, including cephalopods (Mattiello et al., 2010; Romano et al., 2011; Paul et al., 2011). The presence of NOS was revealed by immunostaining using an antibody generated to a peptide of a conserved region in all known animal NOSs.

Both NO and NOS appear localized in the ganglia area and restricted in superficial tissues in the early embryos (stage 18). From stage 20 the cell-specific production of NO is extended in superficial tissues and appears in deep organs and/or structures.

Stage 18

At stage 18, numerous NO positive cells are variously distributed on the embryo with a higher density in the dorsal anterior region between the two eyes around the future mouth (Fig. 2A). This region corresponds to presumptive cerebral ganglia. The mantle area is peripherally stained

(mantle edge) but not in its central part that corresponds to the shell sac depression primordia (shell sac edge + shell sac aperture) (Fig. 2B). Uniform distribution of NO positive cells is detectable in all prospective optic and white body areas (Fig. 2B). At this stage the arms appear to be

arranged as an arm crown: NO positive cells are detected at the basis between the arm buds V and IV corresponding to presumptive pedial ganglia (Fig. 2C). A slight positive signal is also observed above the statocysts in the region corresponding at this stage to the visceral ganglia (Fig. 2A–C). Staining was detectable neither in the brachial ganglia nor in the arm buds and the funnel prospective area, pouches and tube (Fig. 2C).

At stage 18 immunopositivity is detectable in prospective optic and white body areas, in funnel pouches (Fig. 2D). The staining is present along the periphery of the mantle (Fig. 2E), in the visceral ganglia and in the arm buds (Fig. 2F). NOS-like immunoreactivity has not been detected at stage 16.

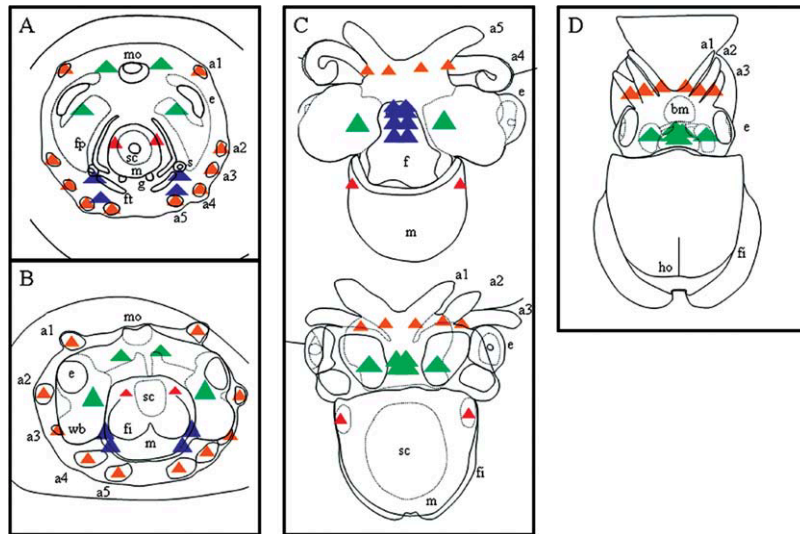


Fig. 1. Schematic representations of embryonic neural territories during *S. officinalis* organogenesis. **A:** Stage 18–19. **B:** Stage 21. **C:** Stage 24 up: ventral side, down: dorsal side. **D:** Stage 29–30. a, arm; bm, buccal mass; e, eye; f, funnel; fi, fin; ft, funnel tube; fp, funnel pouch; g, gill; ho, hoyle organ; m, mantle; mo, mouth; s, statocyste; sc, shell sac; wb, white body. Nervous system color triangles legends: peripheral nervous system (PNS): brachial ganglia (orange) and stellate ganglia (red). Central nervous system (CNS): optic ganglia (pale green) that differentiate into optic lobes from stage 21, cerebral ganglia (dark green); pedial ganglia (pale blue) and visceral ganglia (dark blue) that differentiate and condense into the suboesophageal mass of the brain.

Stages 20–21–22–23

In the dorsal region, NO positive cells are observed in the mouth region in the area of cerebral ganglia (Fig. 1A) corresponding to future dorsal supraesophageal mass of the central nervous system (Fig. 3A, arrow) (Navet et al., 2009). Moreover, several

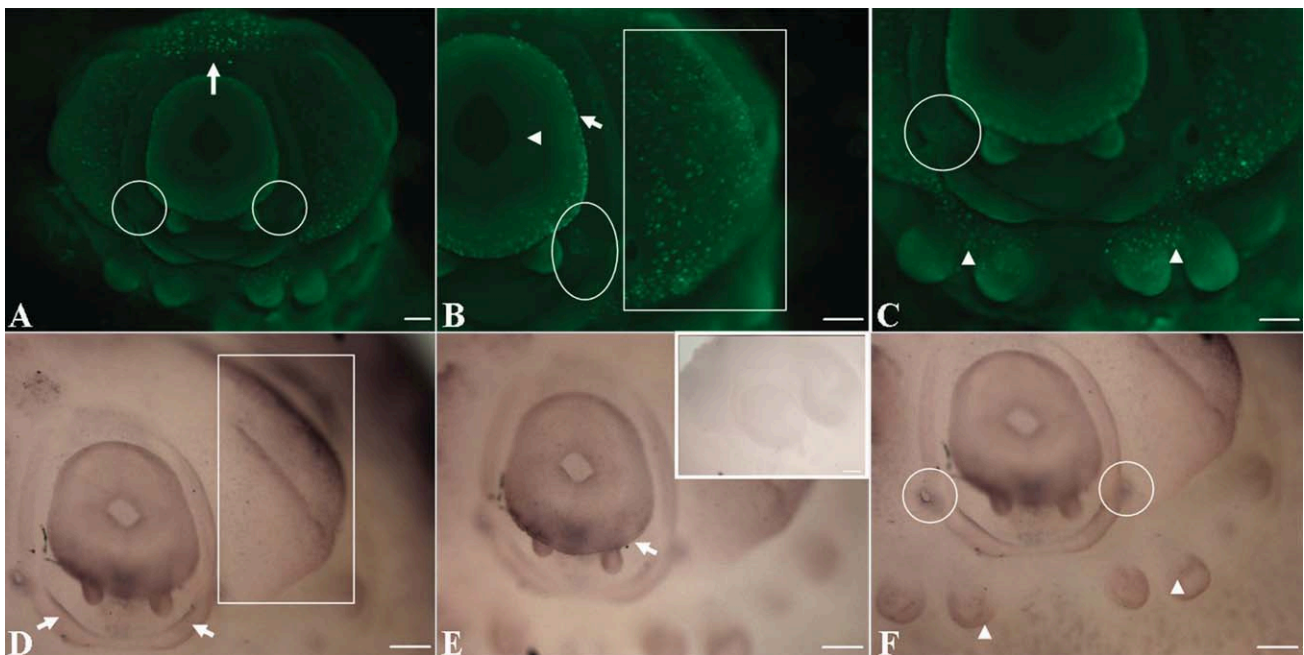


Fig. 2. Nitric oxide (NO) detection and NO synthase (NOS)-like immunoreactivity in *S. officinalis* embryo at stage 18. **A:** NO positive cells in the presumptive cerebral ganglia (arrow) and in the visceral ganglia (circle). **B:** NO positive cells in prospective optic and white body areas (square) and in the visceral ganglia (circle). Arrow: mantle edge. Arrowhead: shell sac depression primordia. **C:** NO positive cells in the visceral ganglia (circle) and in the presumptive pedial ganglia (arrowheads). **D:** Immunopositivity in prospective optic and white body areas (square) and in funnel pouches (arrows). **E:** Immunopositivity in the mantle edge (arrow). Insert: control. **F:** Immunopositivity in the visceral ganglia (circle) and in the arm buds (arrowheads). Scale bars = 200 μm .

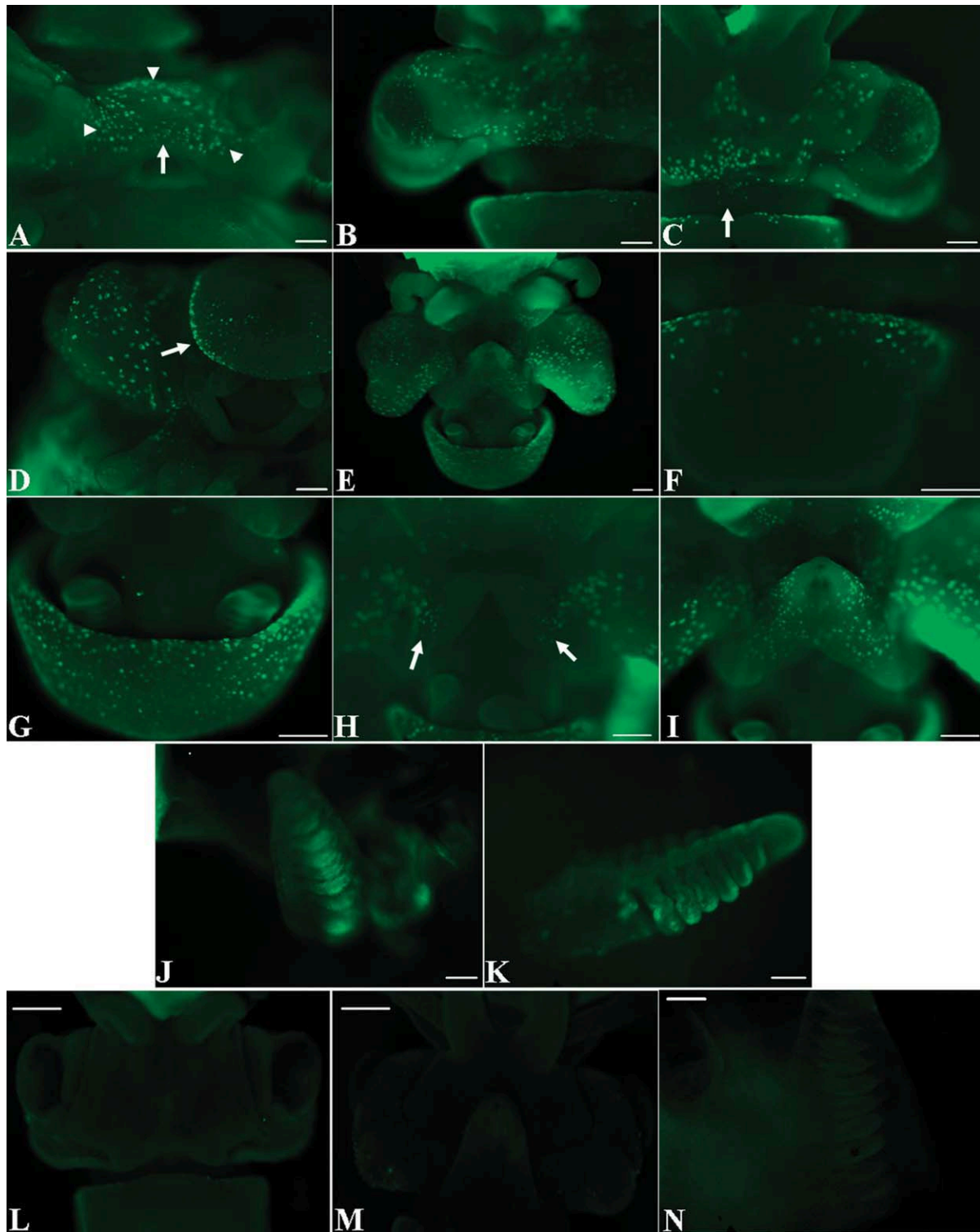


Fig. 3. Nitric oxide (NO) detection in *S. officinalis* organogenesis. **A:** NO positive cells in the area of cerebral ganglia (arrow) and in the epithelial cells (arrowheads) of the central region of the head, stage 20. **B:** NO positive cells extended toward the eyes, stage 22. **C:** Same signal extended toward the eyes. NO positive cells are visible in the nuchal region (arrow), stage 24. **D:** NO positive cells in the lateral edges of the mantle (arrow) and in the optic region of the head, stage 20. **E:** NO positive cells in the ventral head, stage 22. **F:** NO positive cells in the lateral edges of the dorsal mantle, stage 21. **G:** NO positive cells in the ventral mantle and in the gill lamellae, stage 22. **H:** NO Positive cells at the basis of the two elements of the funnel (arrows), stage 21. **I:** NO positive cells in all the funnel surface until the aperture except on the median part, stage 22. **J:** NO positive gill transverse folds, stage 22. **K:** NO positive gill lamellae, stage 24. **L-N:** Control experiments, stage 25 (L) dorsal view; (M) ventral view; (N) gills. Scale bars = 200 μm in A-I, J, K, N, 500 μm in L, M.

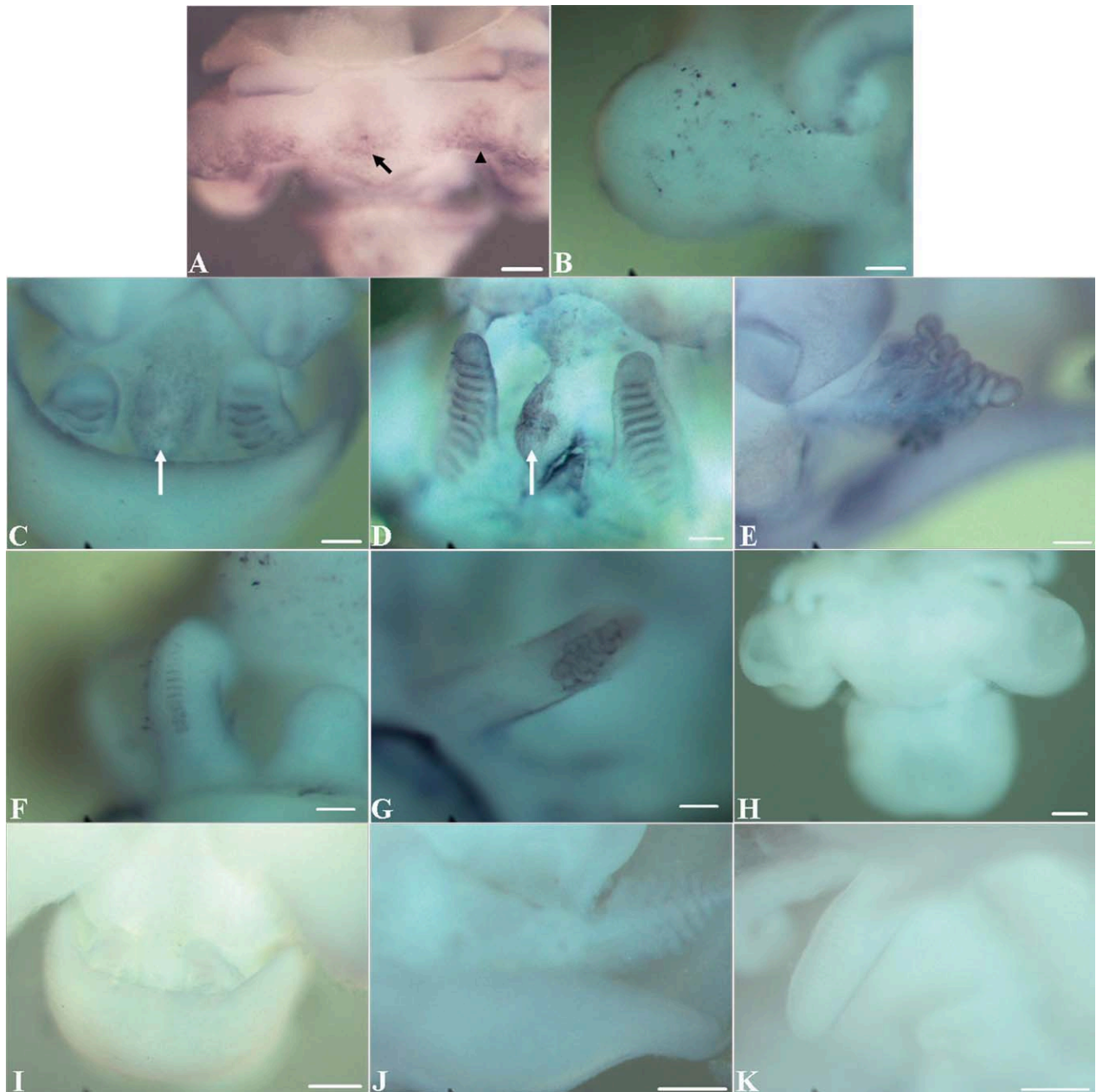


Fig. 4. Nitric oxide synthase (NOS)-like immunoreactivity in *S. officinalis* organogenesis. **A:** Immunopositivity at level of the central region of the head (arrow) and posteriorly to eyes (arrowhead), stage 20. **B:** Immunopositivity in the optic region, stage 20. **C,D:** Immunopositivity in the central region between the gills (arrows) and in gill transverse folds, stage 22. **E:** Immunopositivity in the gill lamellae, stage 24. **F:** Immunopositive arm proximal suckers, stage 20. **G:** Immunopositive suckers of tentacular club, stage 23. **H–K:** Control experiments: dorsal view, stage 25 (H); ventral mantle, stage 23 (I); gill, stage 24 (J); arm suckers, stage 24 (K). Scale bars = 500 μm in H, 200 μm in A,C,I–K, 100 μm in B,D–G.

positive epithelial cells can be detected in this region (Fig. 3A, arrowheads). Positive cells are also located in the posterior part of the optic region (Fig. 3D). From stage 22, the NO fluorescence is localized only in epithelial cells whose distribution is extended toward the eyes (Fig. 3B) until covering totally the eyes at stage 24 (Fig. 3C). Moreover, NO signal is

localized in the nuchal region in which cephalic aorta branches (Fig. 3C). The ventral part of the head shows numerous NO positive cells from stage 20 to 22 (Fig. 3D,E).

In the mantle, NO positive cells are distributed peripherally with higher density in the lateral edges (Fig. 3D). In the dorsal side positive cells are distributed in each lateral part and

are absent in the median central region as well as in the posterior region (Fig. 3F). At stage 22, numerous positive cells appear in the ventral part of the mantle (Fig. 3G), not in the dorsal one where the positive cells remain located on the anterior edges as in the stage 21 (Fig. 3F). The funnel tube folds and the gills do not present any NO positive cells at stage

20 (Fig. 3D). At stage 21, the two elements of the funnel show each at their basis group of NO positive cells; no staining is visible at the anterior extremities in which the folds connect later to close the tube (Fig. 3H). Ventrally, at stage 22, when the funnel tube is formed (by the fusion at its internal face of the two folds), NO positive cells are present and extend in all funnel surface until the aperture except on the median ventral part of the funnel (Fig. 3I). In the gills from stage 22 (Fig. 3G,J), transverse folds corresponding to the delineating of the lamellae appear NO positive; fluorescence cannot be detected as restricted to the cells. At stage 24 NO is localized in the lamellae (Fig. 3K). After treatment with NOS inhibitor L-NAME, NO detection is abolished (Fig. 3L–N).

At stages 20 and 21 NOS immunopositivity is detectable at level of the central region of the head and posteriorly to eyes (Fig. 4A) and optic region (Fig. 4B) resembling the results of NO detection. The immunopositivity in the gills at stages 22 and 24 respectively in the transverse folds (Fig. 4C,D) and in the lamellae (Fig. 4E) overlaps the NO signal. Moreover an intense NOS immunopositivity is distributed in the region between the gills (Fig. 4C,D). In the arms at stage 20, immunopositivity is observed in the proximal suckers not yet differentiated (Fig. 4F), whereas no NO positive suckers have been evidenced in the stages 20 to 23. At stage 23, some of the suckers of the tentacular club, all differentiated, are immunopositive (Fig. 4G) but NO production has been evidenced only at later stages on proximal suckers (stage 27, Fig. 7K). No detectable signal was observed in control experiments with primary antibody omission (Fig. 4H–K).

Stage 26

At stage 26 NO positive cells are variously distributed on the embryo in both dorsal and ventral side. On the head, there are two different NO positive epithelial cell populations. Indeed, on the dorsal side large NO positive cells are located in a triangular area at the centre of the head and in the lateral region bordering the eyes. Small NO positive cells are evidenced on the remaining part of the

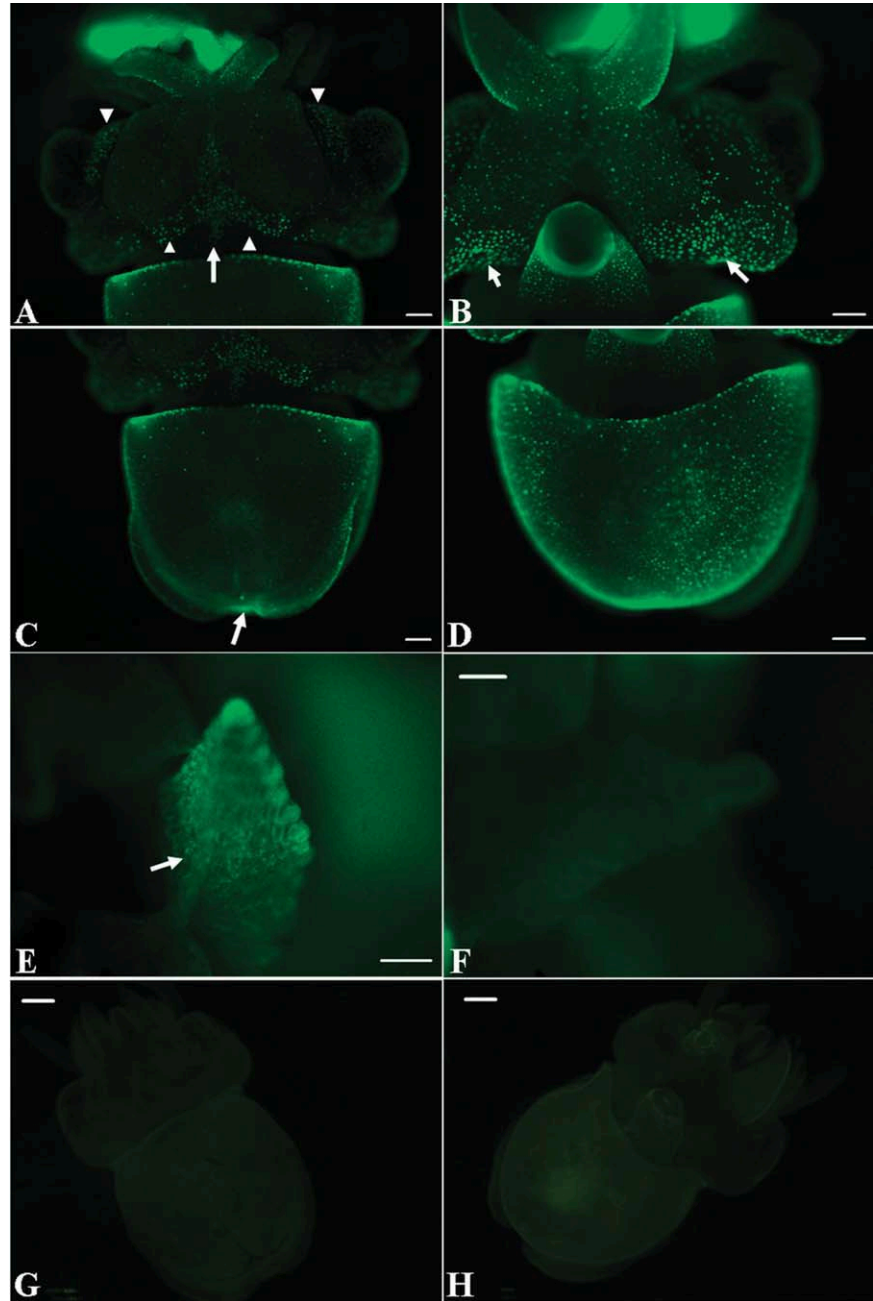


Fig. 5. Nitric oxide (NO) detection in *S. officinalis* embryo at stage 26. **A:** Large NO positive cells located in a triangular area at the centre of the head and in the lateral region bordering the eyes (arrowheads). Small NO positive cells on the remaining part of the head, eyes and the external side of the arms. NO positive cells in the nuchal region (arrow). **B:** Large NO positive cells in two restricted bands (strips) on the ventral head (arrows). **C:** NO positive cells in the lateral edges of the dorsal mantle and in the Hoyle organ (arrow). **D:** NO positive cells in the ventral mantle. **E:** NO positive gill lamellae and afferent vessel (arrow). **F–H:** Control experiments, stage 27 (F), gill; (G), dorsal view; (H), ventral view. Scale bars = 500 μm in A,C,G,H; 200 μm in B,D–F.

head, on the eyes and the external side of the arms (Fig. 5A). Moreover, NO signal is localized in the nuchal region in which cephalic aorta branches (Fig. 5A). On the ventral side of the head, large positive cells

are located in two restricted bands (strips) on the posterior region except in the central part behind the funnel (Fig. 5B). The funnel continues to show NO positive cells equally distributed except in the median part as

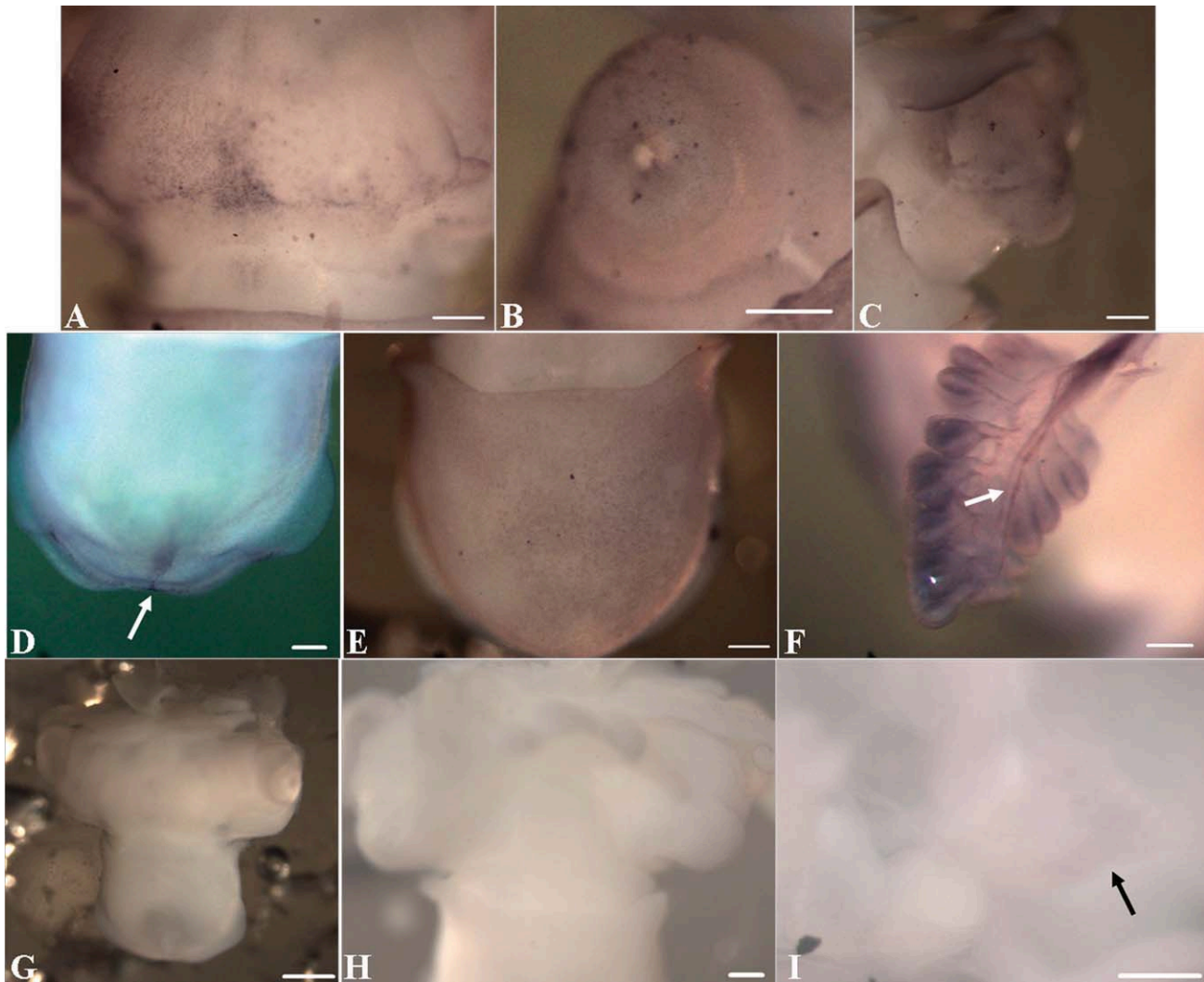


Fig. 6. Nitric oxide synthase (NOS)-like immunoreactivity in *S. officinalis* embryo at stage 26. **A:** Immunopositivity in a triangular area at the centre of the dorsal head. **B:** Immunopositivity on the eye. **C:** Immunopositivity on the ventral head. **D:** A weak immunopositivity in the Hoyle organ (arrow). **E:** Immunopositivity in the ventral mantle. **F:** Immunopositivity in gill lamellae and afferent vessel (arrow). **G–I:** Control experiments. **G,** dorsal view; **H,** ventral view; **I,** gill (arrow). Scale bars = 500 μm in **G**; 200 μm in **A–E,H,I**; 100 μm in **F**.

in the previous stages (Fig. 5B). The dorsal and ventral parts of the mantle show different densities: the NO positive cells are located only at apical and lateral edge of the dorsal mantle, similar to the stage 24, whereas numerous NO-positive cells are distributed in overall ventral mantle (Fig. 5C,D). Moreover, on the dorsal mantle a weak signal begins to appear in the Hoyle organ (Fig. 5C). In the gills the fluorescent signal persists in the more differentiated lamellae and also appears in the afferent vessels as punctuated signal (Fig. 5E). Treatment of embryos with NO scavenger [2-(4-Carboxyphenyl)-4,4,5,5-tetramethylimidazole-1-oxyl-3-oxide] (c-PTIO) abolishes NO detection (Fig.

5F–H). In the dorsal head NOS-like immunopositivity resembles the NO pattern, being localized, as strong signal, in a triangular area at the centre of the head and, as a more dispersed signal, in the remaining part of the head and eyes (Fig. 6A,B). Immunopositivity is localized in the ventral head at level of optic region and in the arms and funnel (Fig. 6C). On the dorsal mantle a weak immunopositive signal in the Hoyle organ closely resembles the NO fluorescence (Fig. 6D). NOS-like immunopositivity on the ventral mantle and gill overlap the NO pattern (Fig. 6E,F). Control experiments performed in the absence of primary antibody show no signal (Fig. 6G–I).

Stages 27–28–29

NO production appears more regionalized in the superficial cells in the late embryonic phase, in which the embryo has already reached the final adult conformation, than in the early developmental phases. In the dorsal side of head, at stages 27, 28 and 29, the positive cells become localized in two specific regions situated in a posterior area of the eyes and extend toward the junction between head and mantle (Fig. 7A). These cells could be epidermal cells as they are superficial and numerous. The median part does not show any positive cells. On the ventral side the large positive cells observed in the posterior part at stage

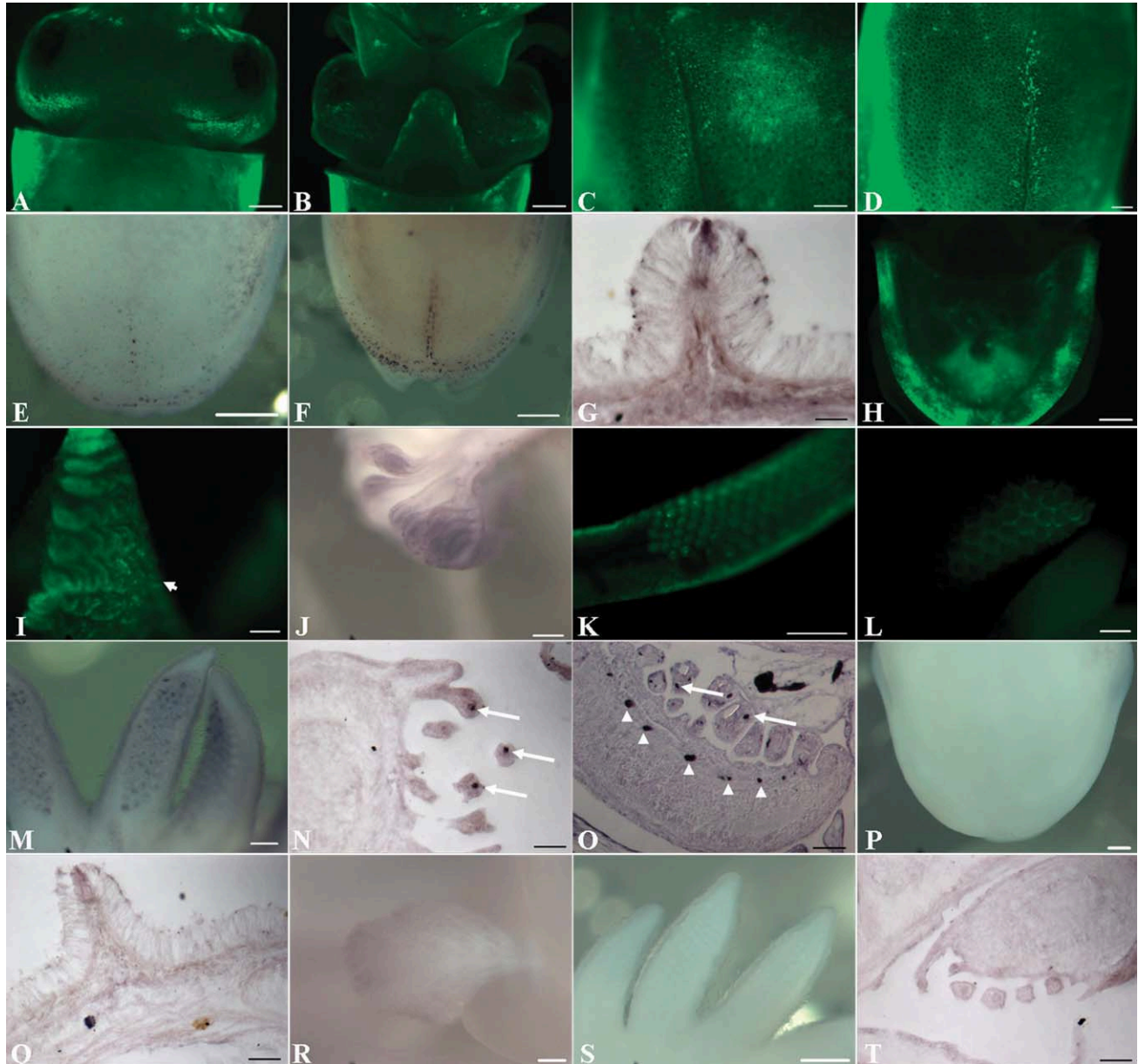


Fig. 7. Nitric oxide (NO) detection and NO synthase (NOS)-like immunoreactivity at late embryonic stages of *S. officinalis*. **A:** NO positive cells in the dorsal head, stage 28. **B:** NO positive cells in the ventral head, stage 28. **C:** NO positive cells in the Hoyle organ, stage 28. **D:** NO positive cells in the Hoyle organ, stage 29. **E:** Immunopositivity in the Hoyle organ, stage 28. **F:** Immunopositivity in the Hoyle organ, stage 29. **G:** Immunopositivity in the Hoyle organ section, stage 28. **H:** NO positive cells in the ventral mantle. Autofluorescence in the digestive bag, stage 28. **I:** NO positive gill lamellae and afferent vessel (arrow), stage 28. **J:** Immunopositive gill lamellae, stage 29. **K:** NO positive proximal suckers of the tentacular club, stage 27. **L:** NO positive distal suckers of the arms, stage 28. **M:** Immunopositive arm suckers, stage 27. **N:** Immunopositive arm suckers on sections (arrows), stage 27. **O:** Immunopositivity on sections in the suckers of the tentacular club (arrows) and in the nervous projections (arrowhead), stage 28. **P–T:** Control experiments. P, Hoyle organ; Q, Hoyle organ section; R, gill; S, arm suckers; T, arm suckers section. Scale bars = 500 μm in A,B,E,F,H; 200 μm in C,D,K,P,R,S; 100 μm in I,J,L,M,O; 50 μm in G,N,Q,T.

26 (see Fig. 5B) do not produce any more NO, whereas more NO producing cells, probably epidermal ones, appear in the anterior region (Fig. 7B). In the posterior region, in the Hoyle organ some specific NO positive cells are distributed with a higher density in the distal part of the midline at stage 28 (Fig. 7C). The number

of cells producing NO extends toward anterior region along the median line at stage 29 (Fig. 7D). The NO production is supported by immunostaining results on whole-mount and on sections (Fig. 7E–G). NOS is evidenced in the same mantle area in the Hoyle organ, both in the median line and laterally following the typical anchor

shape of the organ. The density of the immunopositive cells increases from stage 28 to 29 (Fig. 7E,F). In the ventral side of the mantle NO fluorescence begins to decrease in the central part and becomes restricted on the peripheral strip (Fig. 7H). A low internal signal observed in the digestive bag (Fig. 7H) is attributable to

autofluorescence as shown in control experiments. In the gills, the NO signal as well as NOS-like immunopositivity, persist in lamellae and afferent vessel (Fig. 7I,J). The proximal suckers of the tentacular club and the distal suckers of the arms show NO production (Fig. 7K,L). These signals are supported by immunostaining in the suckers of arms on whole-mount (Fig. 7M) and section (Fig. 7N) as well as tentacular club section (Fig. 7O). In this latter, in addition to the signal in the suckers, immunopositivity is also detectable at level of nervous projections. No detectable signal was observed in control experiments with primary antibody omission (Fig. 7P–T).

NOS Expression During *S. officinalis* Development

Temporal expression of *NOS* during development was followed by real-time PCR (ovocyte, stages 14–30) using primers located downstream the 18 nucleotides insert and which amplify both *SoNOSa* and *SoNOSb*, the two splicing forms identified in the adult (Scheinker et al., 2005). *NOS* expression significantly changes during development compared with that of 16S ribosomal RNA gene (*RPS16*), whose expression remains constant in all the stages examined. In particular, *NOS* expression increases from stages 18 to 22 and then reaches a maximum level of expression at stage 26, as reflected by the decrease of Ct values at these stages (Fig. 8).

DISCUSSION

The results of this study show for the first time that NO is endogenously synthesized in all developmental stages of *S. officinalis* embryos, as revealed by NO and NOS enzyme detection as well as by monitoring *NOS* expression levels after real-time PCR. NO production is very localized and restricted to some regions even if in the apparently same tissues. This production is transitory and is mainly correlated to the presence of NOS, the enzyme responsible of gas formation. In the early stages of organogenesis (stage 18) the pattern of endogenous NO localization overlaps that of NOS distribution in the peripheral mantle,

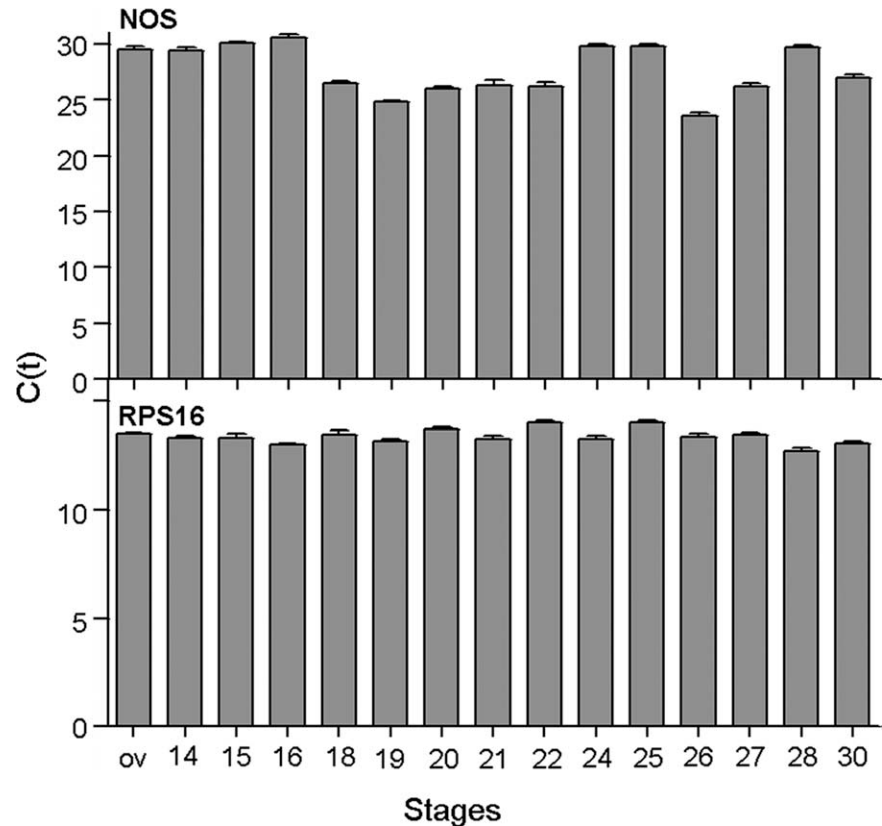


Fig. 8. Temporal expression of *NOS* and *RPS16* during *S. officinalis* development. mRNA levels were measured by real-time polymerase chain reaction from cDNA templates prepared from ovocytes (ov) and embryos at the indicated developmental stages. Data in histograms are reported as mean \pm SD.

prospective optic and white body areas and in specific arms. At subsequent stages (20–21 and 26) this correspondence is maintained in different regions of the head (the central region of the head, and subsequently in the dorsal triangular area at the centre of the head, in the lateral region bordering the eyes and on the eyes). Also in the gills and Hoyle organ NO fluorescence and NOS immunostaining overlap during development. At stage 27 both NO and NOS are present in the suckers of the tentacles and arms. On the contrary, there is no correspondence between the two stainings in the arms and tentacles at least at stages 20/23 (Fig. 9). Indeed, although the arm suckers contain the protein NOS, they do not seem to produce the gas probably due to NOS regulation at posttranslational level. This process has been described to occur during the development of *Drosophila melanogaster* and *L. stagnalis* and has been attributed to the formation of inactive NOS het-

erodimers (Stasiv et al., 2001; Korneev and O'Shea, 2002). The enzyme accumulated during development may be used for a latter production of NO and further experiments will be necessary to address this aspect.

In *Sepia* embryos NO production appears to be very dynamic concerning different cells, different stages of cells of superficial tissues as well as internal tissues and organs (Fig. 9).

Neural System

In *Sepia*, the nervous system is organized as the CNS (the brain) from sparse ganglia before hatching. NO is produced only in the first steps of *Sepia* embryo organogenesis (18–20) in almost all the ganglia area leading later to the CNS. This step corresponds to a crucial phase of differentiation as shown by Baratte and Bonnaud (2009). At the next stages (20 to 22) proliferation occurs, the ganglia grow and displace toward the anterior part of the animal, condense into a

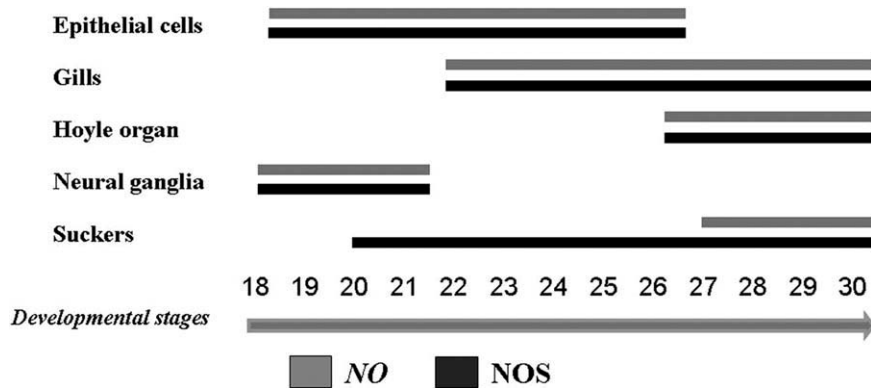


Fig. 9. Schematic representation of nitric oxide (NO) and NO synthase (NOS) localization in different structures during *S. officinalis* development. There is overlapping between NO fluorescence and NOS immunostaining in epithelial cells, gills, Hoyle organ and neural ganglia in all developmental stages. In arm and tentacle suckers the correspondence between the two stainings is maintained in the stages 27–30 and it is not observed at stages 20–26.

brain and the connection takes place with functional differentiation of the lobes, from stages 24 to 30 (Fig. 1). Our finding that when the ganglia have begun to migrate (stage 21) do not produce anymore NO led us to suggest that the gas does not seem to have a role in proliferation of nervous cells but rather in sensorial superficial cells. On this basis, the developmental window where NO might act is very narrow, it is restricted to the first step of neural differentiation. This finding is in line with the differentiation role of NO in several neural in vitro and in vivo models (Contestabile and Ciani, 2004). Considering late stage, the involvement of NO in peripheral nervous system may be inferred by NOS localization in the transversal section of the tentacle where suckers nervous projections are detected (Fig. 70).

Ciliary/Sensory Cells

The dynamic pattern of NO localization in superficial tissues from stage 18 to 27 can be attributed to different type of cells. The NO positive cells in the head and mantle of embryos from stage 18 to 23 (Figs. 2B, 3E–G) correspond to ciliated cells with long hair (Arnold and Williams-Arnold, 1980; Boletzky, 1982). As development proceeds this correspondence is not so straightforward. At stage 26 some of the NO positive cells (Fig. 5A–D) appear to be deeper than the large ciliated cells and may correspond to sensory cells. Of interest, the ciliature

pattern in squid embryos is composed of both paddle elongated ciliated cells and ciliary bands, with very short hairs (Arnold and Williams-Arnold, 1980). These last have been described in *Sepia* embryo only in the region of the Hoyle organ and in late developmental stages. These differences between *Sepia* and *Loligo* embryos are probably due to (1) a different hatching process because of the envelopes more difficult to cross for squids (2) a different lifestyle of sepia and squid juveniles, being the first benthonic and the second planktonic (Boletzky, 1982). Regarding ciliary cells, it seems that NO production is evidenced in long ciliary cells, not in short ciliary bands near the Hoyle organ. The presence of NO could be related to the cilia beating in close analogy with the reported finding that NO regulates the ciliary beating in *Helisoma trivolvis* embryos (Cole et al., 2002) as well as in mammalian cells (Uzlaner and Priel, 1999; Li et al., 2000). In *Sepia* as for squid, the ciliary beating is a process essential for the fluid circulation inside the chorion, preventing accumulation of excretory products and facilitating respiratory exchange (Arnold and Williams-Arnold, 1980; Fioroni, 1990). Moreover, this process also contributes to hatching.

In the case of sensory cells, the finding that the production of NO is maintained during all development, with a larger distribution in the first stage, led us to hypothesize a role of NO in differentiation and maintaining these cells as essential for the perception of

environment after hatching. At later stages (28–29) the NO positive cells appear localized in the Hoyle organ. This organ consists of two different types of cells. The α cells that function as adhesive cells and δ cells containing lytic enzymes necessary to digest the chorion (Fioroni, 1990; Budelmann et al., 1997). The presence of NOS in the anchor shape organ may be related to the chemical process occurring at hatching.

Gills

Both NO and NOS have been detected in the gills at different developmental stages: in the early stages (22–24) when differentiation processes occur in lamellae and in vascular system connection, and in subsequent stages (26–28) when the gills take over the respiration. In cephalopods the gills actively participate in osmoregulation and urine production (Schipp and Boletzky, 1975). In this regard, the presence of Na^+/K^+ -ATPase has been reported in the internal transport-active epithelium of the gills in *S. officinalis* (Hu et al., 2010; Donaubaer, 1981). The functioning of this pump in late embryos is of great importance in regulating acid-base disturbances due to high pCO_2 and low pH values detected inside the egg capsule as hatching approaches (Gutowska and Melzner, 2009; Gutowska et al., 2010). Considering that NO has been reported to affect Na^+/K^+ -ATPase activity in the Atlantic salmon (Ebbesson et al., 2005), a possibility remains that in *Sepia* NO may act on this pump and further colocalization studies will be necessary to prove this hypothesis. Moreover, the presence of NO and NOS in differentiating gills as well as in afferent vessels suggests the possible involvement of the gas in important processes, including morphogenesis and blood circulation. This latter hypothesis is congruent with the vasodilatory role of NO in adult *Sepia* (Schipp and Gebauer, 1999).

Overall these studies represent the first detailed description of NO and NOS pattern during cephalopod development, revealing that NO is produced in different structures characterized by specific functions. The

results provide the basis for future functional studies directed to increase our knowledge of this new developmental model system.

EXPERIMENTAL PROCEDURES

Embryo Collection

All animal procedures were in compliance with the guidelines of the European Union (directive 86/609) and additional procedures for cephalopods recommended in Boyle (Boyle, 1991). Fertilized eggs were laid by *S. officinalis* females after mating with adult males in the tanks of the service marine resources at the Zoological Station. The eggs were allowed to develop in oxygenated sea water (SW) at 20°C. The embryos are protected by several black envelopes surrounding the chorion. They constitute an interface with the environment the exchanges being limited. Three phases of organogenesis are determined: a disk shaped stage (stages 14 to 19), an expansion stage (stages 20 to 22) and a straightening up stage (22–29). Before the beginning of organogenesis, the chorion is linked to the embryo. As the embryo grows, the chorion separates and the space progressively fills with perivitelline fluid. Until hatching the fluid increases probably by ion and water exchanges with environment and the envelopes become thin. From eggs batches, individual eggs were detached and embryos were collected after removing the numerous surrounding envelopes. Embryos belonging to different stages were selected according to the developmental landmarks established by Lemaire (1970) and were examined for NO detection, immunohistochemistry and real-time PCR.

Chemicals

Nitro blue tetrazolium (NBT) and 5-Bromo-4-chloro-3-indolyl phosphate (BCIP) were obtained from Roche Diagnostics S.p.A. (Monza, Italy). 4-amino-5-methylamino-2',7'-difluorofluorescein diacetate (DAF-FM-DA) (10 mM stock in DMSO) from Molecular Probes was purchased from Invitrogen (S. Giuliano Milanese, Italy). [2-(4-Carboxyphenyl)-4,4,5,5-tetramethylimidazole-1-oxyl-3oxide] (c-PTIO) (10 mM stock in SW)

and biotinylated anti-rabbit IgG, VECTASTAIN ABC-AP kit were obtained from Vinci-Biochem (Vinci, Italy).

NO Detection

NO localization was performed starting from stage 18 to 29 using DAF-FM-DA. In previous stages, the chorion is tightly attached to the embryo and its removal causes embryo damage and hampers subsequent NO detection. The samples were incubated in the dark with 12.5 μ M DAF-FM-DA in filtered SW for 20 min for dye loading. Subsequently, they were washed and incubated in SW for 30 min to allow complete de-esterification of diacetates. Fluorescence was visualized with a Leica stereo-microscope equipped with a digital camera Leica DFC 490 and GFP filters. Images were acquired with Leica application suite software. In control experiments embryos were incubated in sea water in the absence or presence of the NO scavenger 1 mM c-PTIO or the NOS inhibitor 10 mM L-NAME before exposure to the NO indicator DAF-FM-DA. After 5 hr the embryos were safely and fluorescence was detected as described above. At least three embryos at each stage were used for both control and reaction.

Immunohistochemistry

Whole-mount immunohistochemistry was performed on *Sepia* embryos from stage 16 to 29. Starting from stage 20, the chorion has been removed and the embryos were fixed for 1 hr in 4% paraformaldehyde (PFA) in 0.1 M MOPS pH 7.5, 0.5 M NaCl at room temperature. Previous stages were prefixed with chorion in the same PFA solution and then, after chorion removal, the embryos were fixed for other 45 min. After washing in SW for 1 hr, the embryos were post-fixed in 20% acetic acid, 0.1% Tween 20 in PBS for 1 hr and then washed in 0.1% Tween 20 in PBS for 1 hr. Embryos were then permeabilized in 0.2% Triton X-100 in PBS for 45 min. Nonspecific binding was blocked by incubating the embryos in blocking buffer: 20% normal goat serum (NGS) in 0.2% Triton-X 100, 1% bovine serum albumin (BSA) in PBS overnight

at 4°C. As primary antibody, rabbit polyclonal anti-universal NOS (Pierce-ABR, Euroclone, Pero, Milan, Italy), generated to a peptide of a conserved C-terminal region present in all known animal NOS, was used. Incubation with primary antibody at a dilution of 1:500 was carried out in 0.2% Triton-X 100, 1% BSA in PBS overnight at 4°C. After washings in 0.1% Triton-X 100 in PBS for 2 hr, embryos were incubated with secondary antibody, biotinylated anti-rabbit IgG (1:2,500) in 0.1% Triton-X 100 in PBS for 2 hr at 4°C. Embryos were then washed in 0.1% Triton-X 100 in PBS for 2 hr. Staining was performed using VECTASTAIN ABC-AP Reagent (Avidin DH and biotinylated alkaline phosphatase H) and visualized by a Leica stereo-microscope equipped with a digital camera Leica DFC 490. The images were acquired using Leica application suite software. The same protocol was used for the control experiments but with omission of the primary antibody.

For immunohistochemistry on sections, fixed embryos at stages 27/28 were included in OCT. Dry cryostat sections (20 μ m) collected on superfrost slides were washed in 0.1% Tween 20 in PBS for 30 min. Slides were incubated in the blocking solution 5% NGS in PBS for 1 hr and then incubated with rabbit polyclonal anti-universal NOS at a dilution of 1:10,000 in 1% BSA in PBS overnight at 4°C. After washings in PBS for 1 hr, sections were incubated with biotinylated secondary antibody 1:20,000 in PBS for 45 min. Sections were then washed with PBS for 30 min. Staining was performed using VECTASTAIN ABC-AP Reagent and visualized with a Zeiss AxioImager M1 microscope. At least three embryos at each stage were used for both control and reaction.

RNA Extraction and cDNA Synthesis

Each dechorionated developmental stage was collected, frozen in liquid nitrogen and kept at -80°C until use. Total RNA was extracted using TRIzol (Invitrogen) according to manufacturer's instructions. After addition of chloroform/isoamyl alcohol (24:1) (0.2 ml/ml TRIzol) and subsequent

centrifugation at 12,000 rpm for 15 min, RNA was precipitated in the presence of glycogen and isopropyl alcohol. Contaminating DNA was degraded by treating each sample with DNase RNase-free kit (Roche) according to manufacturer's instructions. The quantity and purity of total extracted RNA was estimated monitoring both the absorbance at 260 nm and ratios 260/280 and 260/230 nm by Nanodrop (ND-1000 UV-Vis Spectrophotometer; NanoDrop Technologies). The quality of RNA was evaluated by gel electrophoresis. Intact rRNA subunits (28S and 18S) were observed on the gel indicating minimal degradation of the RNA.

For each sample 600 ng of total RNA was retrotranscribed with iScript cDNA Synthesis kit (Bio-Rad) following the manufacturer's instructions. cDNA was diluted 1:2 with H₂O before the use in real-time PCR experiments.

Real-time PCR

Specific primer sets for each gene were designed on the basis of sequences of 16S ribosomal RNA gene (*RPS16*) and *NOS* gene, available on NCBI website. The following primers were used: *NOS* forward (F9), 5'-GAAAGGCTGGGGC-AGCATGAC-3'; *NOS* reverse (R6), 5'-A-ATCATCTCGACGGTGTTCAGA-3'; *RPS16* forward, 5'-GGTTTGACGAAGGTTTACCTG-3'; *RPS16* reverse, 5'-CGCTGTTATCCCTATGGTAAC-3'. A fragment of 150 bp was amplified for *RPS16* gene, a fragment of 207 bp for *NOS* gene.

Specificity of every amplification reaction was verified by melting curve analysis. The efficiency of each primer pair was calculated according to standard methods curves using the equation $E=10^{-1/\text{slope}}$. Five serial dilutions were set up to determine Ct values and reaction efficiencies for all primer pairs. Standard curves were generated for each oligonucleotide pairs using the Ct values versus the logarithm of each dilution factor. PCR efficiencies were calculated for *RPS16* and *NOS* genes and were found to be 2. Diluted cDNA was used as template in a reaction containing a final concentration of 0.3 μM for each primer and 1 \times FastStart SYBR Green master mix (total volume of 25 μl). PCR

amplifications were performed in a Chromo 4 Real Time Detector (Bio-rad) thermal cycler using the following thermal profile: 95°C for 10 min, one cycle for cDNA denaturation; 95°C for 15 sec and 60°C for 1 min, 40 cycles for amplification; 72°C for 5 min, one cycle for final elongation; one cycle for melting curve analysis (from 60°C to 95°C) to verify the presence of a single product. Each assay included a no-template control for each primer pair. To capture intra-assay variability all RT-qPCR reactions were carried out in triplicate. Fluorescence was measured using Opticon Monitor 3.1 (Biorad). Relative expression ratios above two cycles were considered significant. Experiments were repeated at least twice. Statistical analysis was performed using GraphPad Prism version 4.00 for Windows (GraphPad Software, San Diego, CA).

ACKNOWLEDGMENTS

The authors thank the Molecular Biology Service for real-time PCR experiments and for oligos synthesis, Alberto Macina, and the service "Marine Resources for Research" for assistance with living organisms. L.B. and A.A. were funded by an ASSEMBLE grant agreement and they thank the Stazione Zoologica Anton Dohrn for the facilities during their stay in Naples.

REFERENCES

- Andreakis N, D'Aniello S, Albalat R, Patti FP, Garcia-Fernandez J, Procaccini G, Sordino P, Palumbo A. 2011. Evolution of the nitric oxide synthase family in metazoans. *Mol Biol Evol* 28:163–179.
- Arnold JM, Williams-Arnold LD. 1980. Development of the ciliature pattern on the embryo of the squid *Loligo Pealei*: a scanning electron microscope study. *Biol Bull* 159:102–116.
- Baratte S, Bonnaud L. 2009. Evidence of early nervous differentiation and early catecholaminergic sensory system during *Sepia officinalis* embryogenesis. *J Comp Neurol* 517:539–549.
- Baratte S, Andouche A, Bonnaud L. 2007. Engrailed in cephalopods: a key gene related to the emergence of morphological novelties. *Dev Genes Evol* 217:353–362.
- Bishop CD, Brandhorst BP. 2001. NO/cGMP signaling and HSP90 activity represses metamorphosis in the sea urchin *Lytechinus pictus*. *Biol Bull* 201:394–404.
- Bishop CD, Brandhorst BP. 2003. On nitric oxide signaling, metamorphosis,

and the evolution of biphasic life cycles. *Evol Dev* 5:542–550.

- Bishop CD, Brandhorst BP. 2007. Development of nitric oxide synthase-defined neurons in the sea urchin larval ciliary band and evidence for a chemosensory function during metamorphosis. *Dev Dyn* 236:1535–1546.
- Bishop CD, Bates WR, Brandhorst BP. 2001. Regulation of metamorphosis in ascidians involves NO/cGMP signaling and HSP90. *J Exp Zool* 289:374–384.
- Bishop CD, Pires A, Norby SW, Boudko D, Moroz LL, Hadfield MG. 2008. Analysis of nitric oxide-cyclic guanosine monophosphate signaling during metamorphosis of the nudibranch *Phestilla sibogae* Bergh (Gastropoda: Opisthobranchia). *Evol Dev* 10:288–299.
- Boletzky Sv. 1982. Structure tegumentaire de l'embryon et mode d'eclosion chez les Cephalopodes. *Bull Soc Zool Fr* 107:475–483.
- Boletzky Sv, Erlwein B, Hofmann DK. 2006. The *Sepia* egg: a showcase of cephalopod embryology. *Vie et milieu--Life and environment* 56:191–201.
- Boyle PR. 1991. The UFAW handbook on the care and management of cephalopods in the laboratory. Harlow: Longman.
- Bradley S, Tossell K, Lockley R, McDearmid JR. 2010. Nitric oxide synthase regulates morphogenesis of zebrafish spinal cord motoneurons. *J Neurosci* 30:16818–16831.
- Budelmann BU, Schipp R, Boletzky Sv. 1997. Cephalopoda. In: Harrison FW, Kohn AJ, editors. *Microscopic anatomy of invertebrates*. New York: Wiley-Liss. Volume 6A: Mollusca II, p 119–414.
- Colasanti M, Persichini T, Venturini G. 2010. Nitric oxide pathway in lower metazoans. *Nitric Oxide* 23:94–100.
- Cole AG, Mashkournia A, Parries SC, Goldberg JI. 2002. Regulation of early embryonic behavior by nitric oxide in the pond snail *Helisoma trivolvis*. *J Exp Biol* 205:3143–3152.
- Comes S, Locascio A, Silvestre F, d'Ischia M, Russo GL, Tosti E, Branno M, Palumbo A. 2007. Regulatory roles of nitric oxide during larval development and metamorphosis in *Ciona intestinalis*. *Dev Biol* 306:772–784.
- Contestabile A, Ciani E. 2004. Role of nitric oxide in the regulation of neuronal proliferation, survival and differentiation. *Neurochem Int* 45:903–914.
- Di Cosmo A, Di Cristo C, Palumbo A, d'Ischia M, Messenger JB. 2000. Nitric oxide synthase (NOS) in the brain of the cephalopod *Sepia officinalis*. *J Comp Neurol* 428:411–427.
- Di Cristo C, Fiore G, Scheinker V, Enikolopov G, d'Ischia M, Palumbo A, Di Cosmo A. 2007. Nitric oxide synthase expression in the central nervous system of *Sepia officinalis*: an in situ hybridization study. *Eur J Neurosci* 26:1599–1610.
- Donaubauer HH. 1981. Sodium- and potassium-activated adenosine triphosphatase in the excretory organs of *Sepia officinalis* (Cephalopoda). *Mar Biol* 63:143–150.

- Ebbesson LO, Tipsmark CK, Holmqvist B, Nilsen T, Andersson E, Stefansson SO, Madsen SS. 2005. Nitric oxide synthase in the gill of Atlantic salmon: colocalization with and inhibition of Na⁺,K⁺-ATPase. *J Exp Biol* 208:1011–1017.
- Fiore G, Poli A, Di Cosmo A, d'Ischia M, Palumbo A. 2004. Dopamine in the ink defence system of *Sepia officinalis*: biosynthesis, vesicular compartmentation in mature ink gland cells, nitric oxide (NO)/cGMP-induced depletion and fate in secreted ink. *Biochem J* 378:785–791.
- Fioroni P. 1990. Our recent knowledge of the development of the cuttlefish (*Sepia officinalis*). *Zool Anz* 224:1–25.
- Froggett SJ, Leise EM. 1999. Metamorphosis in the marine snail *Ilyanassa obsoleta*, Yes or NO? *Biol Bull* 196:57–62.
- Grimaldi A, Tettamanti G, Acquati F, Bossi E, Guidali ML, Banfi S, Monti L, Valvassori R, de Eguileor M. 2008. A hedgehog homolog is involved in muscle formation and organization of *Sepia officinalis* (mollusca) mantle. *Dev Dyn* 237:659–671.
- Gutowska MA, Melzner F. 2009. Abiotic conditions in cephalopod (*Sepia officinalis*) eggs: embryonic development at low pH and high pCO₂. *Mar Biol* 156:515–519.
- Gutowska MA, Melzner F, Langenbuch M, Bock C, Claireaux G, Pörtner HO. 2010. Acid-base regulatory ability of the cephalopod (*Sepia officinalis*) in response to environmental hypercapnia. *J Comp Physiol B* 180:323–335.
- Halm MP, Chichery MP, Chichery R. 2003. Effect of nitric oxide synthase inhibition on the manipulative behaviour of *Sepia officinalis*. *Comp Biochem Physiol C Toxicol Pharmacol* 134:139–146.
- Hens MD, Fowler KA, Leise EM. 2006. Induction of metamorphosis decreases nitric oxide synthase gene expression in larvae of the marine mollusc *Ilyanassa obsoleta* (say). *Biol Bull* 211:208–211.
- Hu MY, Sucre E, Charmantier-Daures M, Charmantier G, Lucassen M, Himmerkus N, Melzner F. 2010. Localization of ion-regulatory epithelia in embryos and hatchlings of two cephalopods. *Cell Tissue Res* 339:571–583.
- Hu MY, Tseng YC, Stump M, Gutowska MA, Kiko R, Lucassen M, Melzner F. 2011. Elevated seawater PCO₂ differentially affects branchial acid-base transporters over the course of development in the cephalopod *Sepia officinalis*. *Am J Physiol Regul Integr Comp Physiol* 300:R1100–R1114.
- Korneev S, O'Shea M. 2002. Evolution of nitric oxide synthase regulatory genes by DNA inversion. *Mol Biol Evol* 19:1228–1233.
- Leckie C, Empson R, Becchetti A, Thomas J, Galione A, Whitaker M. 2003. The NO pathway acts late during the fertilization response in sea urchin eggs. *J Biol Chem* 278:12247–12254.
- Leise EM, Kempf SC, Durham NR, Gifondorwa DJ. 2004. Induction of metamorphosis in the marine gastropod *Ilyanassa obsoleta*: 5HT, NO and programmed cell death. *Acta Biol Hung* 55:293–300.
- Lemaire J. 1970. Table de developement embryonnaire de *Sepia Officinalis* L. (Mollusque Céphalopode). *Bull Soc Zool France* 95:773–782.
- Li D, Shirakami G, Zhan X, Johns RA. 2000. Regulation of ciliary beat frequency by the nitric oxide-cyclic guanosine monophosphate signaling pathway in rat airway epithelial cells. *Am J Respir Cell Mol Biol* 23:175–181.
- Mattiello T, Fiore G, Brown ER, d'Ischia M, Palumbo A. 2010. Nitric oxide mediates the glutamate-dependent pathway for neurotransmission in *Sepia officinalis* chromatophore organs. *J Biol Chem* 285:24154–24163.
- Mohri T, Sokabe M, Kyojuka K. 2008. Nitric oxide (NO) increase at fertilization in sea urchin eggs upregulates fertilization envelope hardening. *Dev Biol* 322:251–262.
- Naef A. 1928. Die Cephalopoden (Embryologie). *Fauna Flora Golf Napoli*, monogr. 35–2 [English translation available from Smithsonian Institution Libraries, Washington D.C., 20560, USA].
- Nave S, Bassaglia Y, Baratte S, Martin M, Bonnaud L. 2008. Somatic muscle development in *Sepia officinalis* (cephalopoda - mollusca): a new role for NK4. *Dev Dyn* 237:1944–1951.
- Nave S, Andouche A, Baratte S, Bonnaud L. 2009. Shh and Pax6 have unconventional expression patterns in embryonic morphogenesis in *Sepia officinalis* (Cephalopoda). *Gene Expr Patterns* 9:461–467.
- Palumbo A. 2005. Nitric oxide in marine invertebrates: a comparative perspective. *Comp Biochem Physiol A Mol Integr Physiol* 142:241–248.
- Palumbo A, d'Ischia M. 2007. Nitric oxide biogenesis, signalling and roles in molluscs: the *Sepia officinalis* paradigm. In: Trimmer B, Tota B, editors. *Advances in experimental biology*. London: Elsevier. p 45–64.
- Palumbo A, Di Cosmo A, Poli A, Di Cristo C, d'Ischia M. 1999. A calcium/calmodulin-dependent nitric oxide synthase, NMDAR2/3 receptor subunits, and glutamate in the CNS of the cuttlefish *Sepia officinalis*: localization in specific neural pathways controlling the inking system. *J Neurochem* 73:1254–1263.
- Palumbo A, Poli A, Di Cosmo A, d'Ischia M. 2000. N-Methyl-D-aspartate receptor stimulation activates tyrosinase and promotes melanin synthesis in the ink gland of the cuttlefish *Sepia officinalis* through the nitric oxide/cGMP signal transduction pathway. A novel possible role for glutamate as physiologic activator of melanogenesis. *J Biol Chem* 275:16885–16890.
- Paul DM, Vilas SP, Kumar JM. 2011. A flow-cytometry assisted segregation of responding and non-responding population of endothelial cells for enhanced detection of intracellular nitric oxide production. *Nitric Oxide* 25:31–40.
- Pechenik JA, Cochrane DE, Li W, West ET, Pires A, Leppo M. 2007. Nitric oxide inhibits metamorphosis in larvae of *Crepidula fornicata*, the slippershell snail. *Biol Bull* 213:160–171.
- Peunova N, Scheinker V, Ravi K, Enikolopov G. 2007. Nitric oxide coordinates cell proliferation and cell movements during early development of *Xenopus*. *Cell Cycle* 6:3132–3144.
- Romano G, Costantini M, Buttino I, Ianora A, Palumbo A. 2011. Nitric oxide mediates the stress response induced by diatom aldehydes in the sea urchin *Paracentrotus lividus*. *PLoS ONE* 6:e25980.
- Scheinker V, Fiore G, Di Cristo C, Di Cosmo A, d'Ischia M, Enikolopov G, Palumbo A. 2005. Nitric oxide synthase in the nervous system and ink gland of the cuttlefish *Sepia officinalis*: molecular cloning and expression. *Biochem Biophys Res Commun* 338:1204–1215.
- Schipp R, Boletzky Sv. 1975. Morphology and function of the excretory organs in dibranchiate cephalopods. *Fortschritt Zool* 23:89–111.
- Schipp R, Gebauer M. 1999. Nitric oxide: a vasodilatory mediator in the cephalic aorta of *Sepia officinalis* (L.) (Cephalopoda). *Invert Neurosci* 4:9–15.
- Serfözö Z, Elekes K. 2002. Nitric oxide level regulates the embryonic development of the pond snail *Lymnaea stagnalis*: pharmacological, behavioral, and ultrastructural studies. *Cell Tissue Res* 310:119–130.
- Stasiv Y, Regulski M, Kuzin B, Tully T, Enikolopov G. 2001. The Drosophila nitric-oxide synthase gene (dNOS) encodes a family of proteins that can modulate NOS activity by acting as dominant negative regulators. *J Biol Chem* 276:42241–42251.
- Thavaradhara K, Leise EM. 2001. Localization of nitric oxide synthase-like immunoreactivity in the developing nervous system of the snail *Ilyanassa obsoleta*. *J Neurocytol* 30:449–456.
- Tranguch S, Steuerwald N, Huet-Hudson YM. 2003. Nitric oxide synthase production and nitric oxide regulation of pre-implantation embryo development. *Biol Reprod* 68:1538–1544.
- Tu Y, Budelmann BU. 2000. Effects of nitric oxide donors on the afferent resting activity in the cephalopod statocyst. *Brain Res* 865:211–220.
- Uzlaner N, Priel Z. 1999. Interplay between the NO pathway and elevated [Ca²⁺]_i enhances ciliary activity in rabbit trachea. *J Physiol* 516:179–190.
- Welshhans K, Rehder V. 2007. Nitric oxide regulates growth cone filopodial dynamics via ryanodine receptor-mediated calcium release. *Eur J Neurosci* 26:1537–1547.
- Willmott N, Sethi JK, Walseth TF, Lee HC, White AM, Galione A. 1996. Nitric oxide-induced mobilization of intracellular calcium via the cyclic ADP-ribose signaling pathway. *J Biol Chem* 271:3699–3705.